scientific reports

Check for updates

OPEN

A machine learning based prediction model for short term efficacy of nasopharyngeal carcinoma

Qiulu Zhong[1,4], Xiangde Li[1,4], Qinghua Du[1], Qianfu Liang[1], Danjing Luo[1], Jiaying Wen[1], Haiying Yue[1], Wenqi Liu[1], Xiaodong Zhu[2,3]✉ & Jian Li[1]✉

The radiological dosimetric parameters and clinical features were screened by machine learning to construct a prediction model for the short-term efficacy of locally advanced Nasopharyngeal Carcinoma (LANPC). Patients diagnosed with Nasopharyngeal Carcinoma were retrospectively collected in the study. Twenty-four clinical features and twelve radiological dosimetric features were included. Three machine learning algorithms were used to construct predictive models for the short-term efficacy of LANPC. Kaplan–Meier log-rank method was used to compare the prognosis of patients with different efficacies in the model. The reliability of the model was evaluated using the calibration curve and the area under the curve (AUC). There were 194 patients who met the inclusion criteria. Among the three models being constructed, Random forest (RSF) model showed the best predictive ability, with AUC values of 1.000 in the training group and 0.944 in the test group, followed by XGBoost decision tree (GBDT) model (0.866/0.849) and decision tree (DT) model (0.848/0.783). In RSF model, the 3-year and 5-year overall survival rates of patients in complete remission (CR) group were 98.9% (95% CI 0.9688–1.0000) and 89.7% (95% CI 0.8256–0.9752), respectively.While for patients in non-CR group, the 3-year and 5-year overall survival (OS) rate was 100% (95%CI 1.000~1.000) and 98.8% (95% CI 0.9652–1.0000), respectively. There has statistically significant difference between the two groups ($P = 0.0037$). RSF model constructed by machine-learning algorithm based on radiological dosimetric parameters and clinical characteristics can better predict the short-term efficacy of LANPC, and is an effective tool to evaluate the short-term efficacy of different LANPC patients during treatment.

Keywords Locoregionally advanced nasopharyngeal carcinoma, Short-term efficacy, Machine-learning algorithm, Radiological dosimetric parameters

Abbreviations

AUC	Area under curve
AC	Adjuvant chemotherapy
CI	Confidence interval
CR	Complete remission
CCRT	Concurrent chemoradiotherapy
CTV	Clinical target volume
Dmax	Maximum point dose
Dmin	Minimum point dose
Dmean/average	Mean/average point dose
D1cc	Maximum dose in 1 cubic centimeter
D1%	Minimum dose to 1% volume
DVH	Dose volume histogram
DT	Decision tree

[1]Department of Radiation Oncology, The Second Affiliated Hospital of Guangxi Medical University, Nanning 530000, China. [2]Department of Radiation Oncology, Wuming Hospital of Guangxi Medical University, Nanning 530000, China. [3]Department of Radiation Oncology, Guangxi Medical University Cancer Hospital, Nanning 530000, China. [4]Qiulu Zhong and Xiangde Li contributed equally to this work. ✉email: zhuxdonggxmu@126.com; 13978896800@163.com

ECOG	Eastern cooperative oncology group
GTVnd	Gross tumor volume of node
GTVnx	Gross tumor volume for nasopharynx
GBDT	XGboost decision tree
IMRT	Intensity modulated radiotherapy
IC	Induction chemotherapy
LANPC	Locoregionally advanced nasopharyngeal carcinoma
NPC	Nasopharyngeal carcinoma
OS	Overall survival
PR	Partial remission
PD	Progressive disease
RSF	Random forest
RECIST	Response evaluation criteria in solid tumors
SD	Stable disease

In the era of Intensity Modulated Radiotherapy (IMRT), the 5-year overall survival rate of Locally Advanced Nasopharyngeal Carcinoma (LANPC) has reached 80%[1]. The 2023 edition of the Chinese Society of Clinical Oncology (CSCO) Guidelines for Diagnosis and Treatment of Nasopharyngeal Carcinoma[2] recommends induction chemotherapy combined with concurrent chemoradiotherapy as a Category 1 A recommendation for LANPC, and the GP regimen is one of the preferred options for induction chemotherapy in LANPC[3–5]. In a study by Professor Jun Ma's team at Sun Yat-sen University, the GP regimen combined with concurrent chemoradiotherapy (CCRT) in the treatment of LANPC improved the 5-year failure-free survival rate (FFS) by 14%, but some patients were still unresponsive to treatment, with 20% experiencing relapse or distant metastasis after receiving induction chemotherapy plus concurrent chemoradiotherapy (IC + CCRT)[6]. Therefore, the heterogeneity in treatment response necessitates personalized therapy for different patients. Currently, the most reliable indicators for predicting treatment outcomes are primarily concentrated in the levels of serum Epstein–Barr virus-DNA (EBV-DNA). Previous studies have shown that differences in EBV levels before and after treatment indicate variations in prognosis. A study by Sengar et al.[7] found that patients with high pre-treatment EBV-DNA levels had a shorter Overall Survival (OS) by 26.7 months compared to those with lower EBV-DNA levels. Moreover, if the plasma EBV-DNA level remains higher after treatment compared to the pre-treatment level, it may suggest that the presence of residual tumor, and these patients often have a worse OS[8]. Additionally, several studies have observed that there is a more pronounced difference in OS rates between patients who tested positive for plasma EBV-DNA levels after treatment and those whose post-treatment EBV-DNA levels were undetectable[9–15].In recent years, with the rise of big data and artificial intelligence (AI), many scholars have used bioinformatics databases or AI analysis methods to predict tumor regression after induction chemotherapy, thereby predicting the efficacy of concurrent chemoradiotherapy. Professor Xiaodong Zhu's team[16] evaluated the response of 498 LANPC patients after two cycles of induction chemotherapy using MRI and divided the patients into "good responders" and "poor responders" to construct a nomogram for predicting the efficacy in the concurrent chemoradiotherapy phase. The results showed that this predictive model could accurately forecast the subsequent treatment effects in LANPC patients based on their response evaluation after two cycles of induction chemotherapy, providing a basis for personalized treatment plans in clinical settings. Additionally, the team also collected data from 699 T3-4 N0 Nasopharyngeal Carcinoma patients to construct a nomogram for predicting the selection of treatment strategies for different patients[17]. All these prediction models provide reference value for clinical diagnosis and treatment. However, there are still few studies that use machine learning methods to build models predicting short-term efficacy by integrating clinical characteristics and radiological dosimetric features. Therefore, this paper will retrospectively collect clinical and radiological dosimetric characteristics of LANPC, and employ three machine learning methods to construct predictive models for the short-term efficacy of LANPC.

Results

Clinical and patients characteristics

A total of 789 patients with locally advanced nasopharyngeal carcinoma were collected. According to the inclusion and exclusion criteria, 194 eligible patients were included. After balancing based on efficacy evaluation using the "ROSE" package, the training group consisted of 68 patients evaluated as CR and 69 as non-CR, while the test group included 28 patients evaluated as CR and 29 as non-CR. According to the UICC/AJCC 7 th edition staging, there were 78 patients (40.2%) classified as stage III and 116 patients (59.8%) as stage IVa in the entire cohort. Furthermore, there were 74 (38.1%) cases of T3 patients, and 104 (53.6%) cases of T4 patients. The majority of the patients were male, representing 72.7% (141/194) of the total. Among the enrolled patients, most did not have infiltration of the oropharynx and nasal cavity (172/194, 88.7%; 149/194, 76.8%). There were 142 (73.2%) cases with involvement of one side of the parapharyngeal space, while 127 (65.5%) patients had prevertebral muscle involvement. The proportions of carotid sheath involvement were comparable between those with and without infiltration (102/194, 52.6%; 92/194, 47.4%). Regarding lymph nodes, there were 82 (42.3%) cases with fusion of multiple lymph nodes and 112 (57.7%) cases without fusion, while most patients did not have extracapsular infiltration or liquefactive necrosis of the lymph nodes. Among the included patients, 72 (37.1%) received induction plus concurrent chemoradiotherapy, 93 (47.9%) underwent concurrent chemoradiotherapy, 17 (8.8%) had concurrent chemoradiotherapy followed by adjuvant chemotherapy, and 12 (6.2%) were treated with induction chemotherapy plus concurrent chemoradiotherapy and adjuvant chemotherapy. A total of 14 patients experienced radiation-induced temporal lobe injury, accounting for 7.2% of all enrolled patients. Patients baseline characteristics were shown in Table 1.

Characteristic	Total ($n = 194$)	Training set ($n = 137$)	Test set ($n = 57$)	*P* Value
Gender (%)				0.277
Female	53 (27.3)	41 (29.9)	12 (21.1)	
Male	141 (72.7)	96 (70.1)	45 (78.9)	
Age	46 (19–76)	45.1 (20–70)	46.1 (19–76)	
Clinical stage (%)				0.406
III	78 (40.2)	52 (38.0)	26 (45.6)	
IVa	116 (59.8)	85 (62.0)	31 (54.4)	
T stage (%)				0.706
T1	1 (0.5)	1 (0.7)	0 (0.0)	
T2	15 (7.8)	12 (8.8)	3 (5.3)	
T3	74 (38.1)	50 (36.5)	24 (42.1)	
T4	104 (53.6)	74 (54.0)	30 (52.6)	
N stage (%)				0.149
N0	17 (8.8)	10 (7.3)	7 (12.3)	
N1	66 (34.0)	45 (32.8)	21 (36.8)	
N2	90 (46.4)	63 (46.0)	27 (47.4)	
N3	21 (10.8)	19 (13.9)	2 (3.5)	
Oropharynx invasion (%)				0.607
Yes	22 (11.3)	14 (10.2)	8 (14.0)	
No	172 (88.7)	123 (89.8)	49 (86.0)	
Nasal cavity invasion (%)				0.019
Yes	45 (23.2)	25 (18.2)	20 (35.1)	
No	149 (76.8)	112 (81.8)	37 (64.9)	
Parapharyngeal invasion (%)				0.108
No	37 (19.1)	27 (19.7)	10 (17.5)	
One side	142 (73.2)	96 (70.1)	46 (80.7)	
Bilateral	15 (7.8)	14 (10.2)	1 (1.8)	
Prevertebral muscle invasion (%)				1.000
Yes	127 (65.5)	90 (65.7)	37 (64.9)	
No	67 (34.5)	47 (34.3)	20 (35.1)	
Carotid sheath area invasion (%)				0.643
Yes	102 (52.6)	74 (54.0)	28 (49.1)	
No	92 (47.4)	63 (46.0)	29 (50.9)	
Medial pterygoid muscle invasion (%)				0.327
No	89 (45.9)	60 (43.8)	29 (50.9)	
One side	101 (52.1)	73 (53.3)	28 (49.1)	
Bilateral	4 (2.0)	4 (2.9)	0 (0.0)	
Lateral pterygoid muscle invasion (%)				0.520
Yes	45 (23.2)	34 (24.8)	11 (19.3)	
No	149 (76.8)	103 (75.2)	46 (80.7)	
Infratemporal fossa invasion (%)				0.709
Yes	14 (7.2)	11 (8.0)	3 (5.3)	
No	180 (92.8)	126 (92.0)	54 (94.7)	
Intracranial invasion (%)				1.000
Yes	15 (7.7)	11 (8.0)	4 (7.0)	
No	179 (92.3)	126 (92.0)	53 (93.0)	
Cavernous sinus invasion (%)				0.522
No	139 (71.6)	97 (70.8)	42 (73.7)	
One side	52 (26.8)	37 (27.0)	15 (26.3)	
Skull base invasion (%)				0.234
Yes	151 (77.8)	103 (75.2)	48 (84.2)	
No	43 (22.2)	34 (24.8)	9 (15.8)	
Cranial nerve invasion (%)				0.223
Yes	7 (3.6)	3 (2.2)	4 (7.0)	
No	187 (96.4)	134 (97.8)	53 (93.0)	
Lymph nodes invade to the lower neck (%)				0.048
Continued				

Characteristic	Total ($n = 194$)	Training set ($n = 137$)	Test set ($n = 57$)	*P* Value
Yes	12 (6.2)	12 (8.8)	0 (0.0)	
No	182 (93.8)	125 (91.2)	57 (100.0)	
Lymph node fusion (%)				0.252
Yes	82 (42.3)	62 (45.3)	20 (35.1)	
No	112 (57.7)	75 (54.7)	37 (64.9)	
Lymph node edge enhancement (%)				0.086
Yes	15 (7.7)	14 (10.2)	1 (1.8)	
No	179 (92.3)	123 (89.8)	56 (98.2)	
Lymph node necrosis (%)				0.064
Yes	38 (19.6)	32 (23.4)	6 (10.5)	
No	156 (80.4)	105 (76.6)	51 (89.5)	
Therapeutic evaluation (%)				1.000
CR	96 (49.5)	68 (49.6)	28 (49.1)	
Non-CR	98 (50.5)	69 (50.4)	29 (50.9)	
Status (%)				0.122
Alive	183 (94.3)	132 (96.4)	51 (89.5)	
Dead	11 (5.7)	5 (3.6)	6 (10.5)	
Treatment method				0.935
IC + CCRT	72 (37.1)	50 (36.5)	22 (38.6)	
CCRT	93 (47.9)	66 (48.2)	27 (47.4)	
CCRT + AC	17 (8.8)	13 (9.5)	4 (7.0)	
IC + CCRT + AC	12 (6.2)	8 (5.8)	4 (7.0)	
Temporal lobe necrosis				0.326
Yes	14 (7.2)	12 (8.8)	2 (3.5)	
No	180 (92.8)	125 (91.2)	55 (96.5)	

Table 1. The baseline characteristics in patients.

Variable	Training set $n = 137$	Test set $n = 57$	*P* value
PGTVnx_Dmax (cGy)	8066.23	8191.03	0.302
PGTVnx_Dmin (cGy)	5926.21	5862.49	0.695
PGTVnx_Daverage (cGy)	7319.84	7392.43	0.446
PGTVnx_D95 (cGy)[a]	6878.78	6915.96	0.694
PGTVnx_Volume (cm^3)	61.95	63.5	0.83
PGTVnd_L_Dmax (cGy)	7620.63	7805.7	0.222
PGTVnd_L_Dmin (cGy)	5617.15	5767.84	0.66
PGTVnd_L_Daverage (cGy)	7033.65	7162.89	0.502
PGTVnd_L_Volume (cm^3)	17.97	13.64	0.431
PGTVnd_R_Dmax (cGy)	7393.95	7155.97	0.348
PGTVnd_R_Dmin (cGy)	5363.63	5607.1	0.498
PGTVnd_R_Daverage (cGy)	6958.18	7015.95	0.768

Table 2. The radiation dosimatry parameters in training cohort and test cohort. [a]PGTVnx_D95, the minimum absorbed dose that covers 95% of the target volume. There was no significant difference between the two groups.

Characteristics of DVH features

All the enrolled Nasopharyngeal Carcinoma patients underwent radiotherapy in the manner described in the above methods. In our study, there were 12 DVH features extracted from the initial radiation treatment plans, including PGTVnx Dmax, PGTVnx Dmin, PGTVnx Daverage, PGTVnx D95, PGTVnx Volume, PGTVnd_L Dmax, PGTVnd_L Dmin, PGTVnd_L Daverage, PGTVnd_L Volume, PGTVnd_R Dmax, PGTVnd_R Dmin and PGTVnd_R Daverage. There was no significant difference between training cohort and test cohort (Table 2).

Machine learning-based DT model for predicting short-term outcomes in LANPC

Based on the data characteristics of this study, we chose to use "rpart" package to build the model. There was no statistically significant difference between two groups (Table 1). As shown in Fig. 1A, the most important

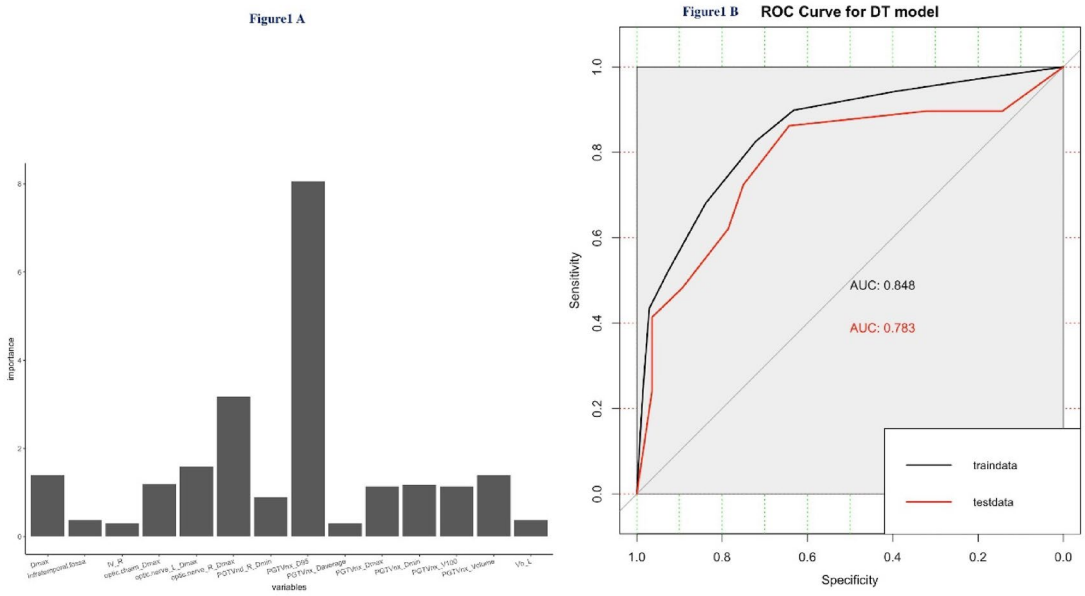

Fig. 1. **A** The important variables of DT model. As shown in **A**, the most important feature was PGTVnx D95, followed by PGTVnd_R Daverage, PGTVnx Volume, PGTVnd_R Dmax and Lateral pterygoid muscle. **B** ROC curve for DT model. The AUC value In the training set was 0.848. While in test cohort, the AUC value was 0.783.

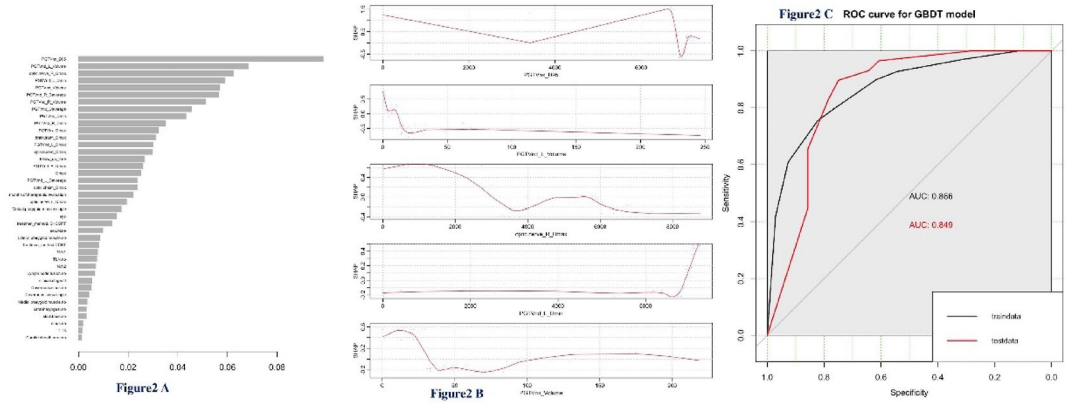

Fig. 2. **A** The important variables for GBDT. **B** The top 5 important variables of GBDT model. From **A** and **B** the most important variable was PGTVnx D95, followed by PGTVnd-L volume, optic nerve-R Dmax, PGTVnd-L Dmin, and PGTVnx volume. **C** ROC curve for GBDT model. The AUC value of GBDT model was 0.866 in training cohort and 0.849 in the test cohort.

feature was PGTVnx D95, followed by PGTVnd_R Daverage, PGTVnx Volume, PGTVnd_R Dmax and Lateral pterygoid muscle. Based on the weight ranking of important features obtained from the classification decision tree and international consensus, we selected the top 5 important features to generate the DT model. Figure 1B shows the ROC curves and AUC values of DT model in both the training and test set to predict the probability to achieve CR at the end of treatment. In the training set, the prediction accuracy of the model was 0.7737 (95%CI: 0.6945, 0.8408), the sensitivity was 0.7206, the specificity was 0.8261, and the AUC value was 0.848. While in test cohort, the accuracy of the model was 0.7368 (95%CI: (0.6034, 0.8446), the sensitivity was 0.7500, the specificity was 0.7241, and the AUC value was 0.783 (Fig. 1B).

Machine learning-based GBDT model for predicting short-term outcomes in LANPC

We used "XGboost" algorithm to built another machine learning-based GBDT model, which is an addition model based on boosting enhancement strategy. The importance of each variable was obtained from the algorithm, with PGTVnx D95 being the most important, followed by PGTVnd-L volume, optic nerve-R Dmax, PGTVnd-L Dmin, and PGTVnx volume (Fig. 2A,B). GBDT model was constructed using these five selected variables. In this model, the accuracy for the training group was 0.7883 (0.7103, 0.8534), with a sensitivity of

Figure 3A Figure 3B Figure 3C

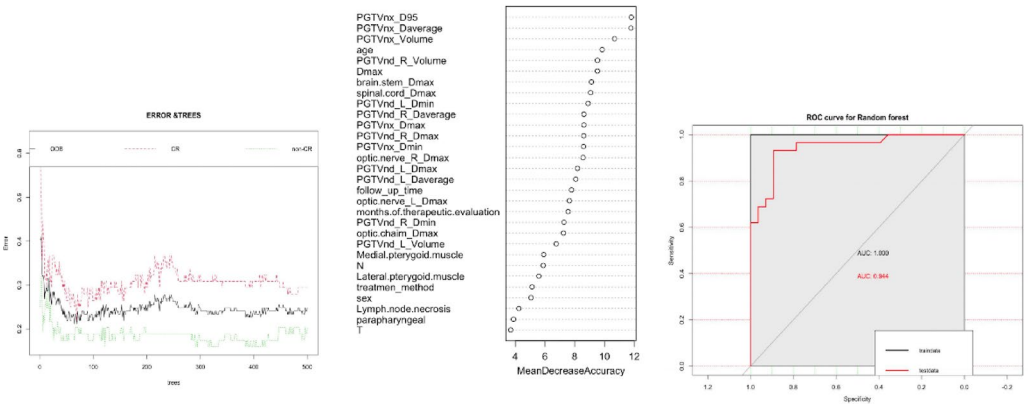

Fig. 3. **A** The OOB error rate to assess the quality of the short-term effects prediction for LANPC in the RSF model. The lowest OOB error rate of 24.82% with an mtry value of 3 and the ntree value of 500. **B** The important variables of RSF model. The top five important variable factors were PGTVnx D95, PGTVnx Daverage, PGTVnx volume, age, and PGTVnd_R volume by using randomForest method. **C** ROC curve for RSF model. The AUC value of RSF model is 1.000 in training set, and of 0.944 in test set.

	Predicting the short-term outcomes of LANPC			
	Accuracy	**Sensitivity**	**Specificity**	**AUC value**
DT model				
training cohort	0.7737 (95% CI: 0.6945, 0.8408)	0.7206	0.8261	0.848
test cohort	0.7368 (95% CI: 0.6034, 0.8446)	0.7500	0.7241	0.783
GBDT model				
training cohort	0.7883 (95% CI: 0.7103, 0.8534)	0.8235	0.7536	0.866
test cohort	0.807 (95% CI: 0.6809, 0.8995)	0.7857	0.8276	0.849
RSF model				
training cohort	1.000 (95% CI: 0.9734, 1)	1.000	1.0000	1.000
test cohort	0.8947 (95% CI: 0.7848, 0.9604)	0.8929	0.8966	0.944

Table 3. Comparison of the predictions of the three models in the training group and the test group.

0.8235 and a specificity of 0.7536, and an AUC value of 0.866. The test group had an accuracy of 0.807 (95% CI: 0.6809, 0.8995), a sensitivity of 0.7857, a specificity of 0.8276, and the AUC value was 0.849 (Fig. 2C).

Machine learning-based RSF model for predicting short-term outcomes in LANPC

The random forest method was used to construct the RSF model. Similarly, we splited the entire dataset into two separate datasets, 70% into the training set (N= 137) and 30% into the test group (N= 57). There was no significant statistical significance in the two groups (Table 1). Subsequently, we obtained the lowest OOB error rate of 24.82% with an m_{try} value of 3 and the ntree value of 500 (Fig. 3A) in the training set. Then, based on the importance and relevance of the variables, the top five important variable factors were determined. Among them, PGTVnx D95 was the most important, followed by PGTVnx Daverage, PGTVnx volume, age, and PGTVnd_R volume (Fig. 3B). Based on these variables, we constructed the RSF model. Figure 3C displays the prediction outcomes for the training and test groups. The accuracy of RSF model for the training set was 1.000 (0.9734, 1), with a sensitivity and specificity of 1.000 each, and an AUC value of 1.000. The test cohort had an accuracy of 0.8947 (95% CI: 0.7848, 0.9604), a sensitivity of 0.8929, a specificity of 0.8966, and an AUC value of 0.944. Table 3 illustrates the probabilities of achieving CR at the end of treatment for LANPC as predicted by these three machine learning-based predictive models.

Table 3 illustrates the probabilities of achieving CR at the end of treatment for LANPC as predicted by these three machine learning-based predictive models. From the results, the RSF model had superior predictive abilities than DT model and GBDT model.

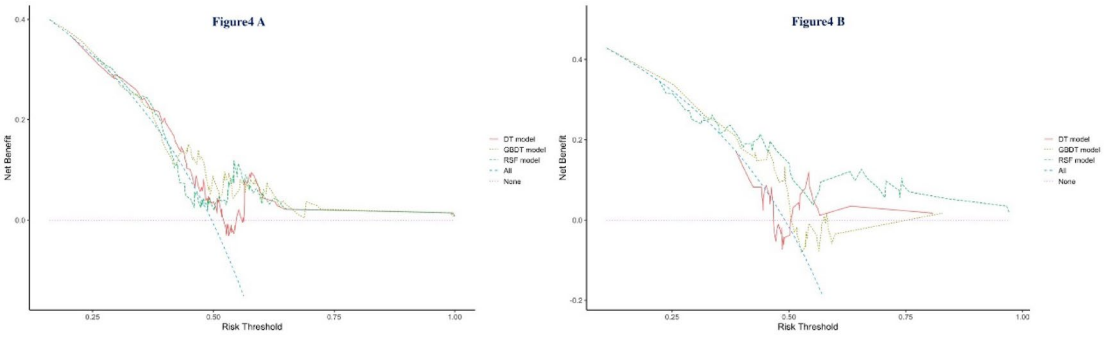

Fig. 4. **A** Decision curves analysis of three models in training cohort, **B** Decision curves analysis of three models in test cohort. RSF model had superior predictive abilities for clinical decision-making than the DT and GBDT models both in the training and test groups.

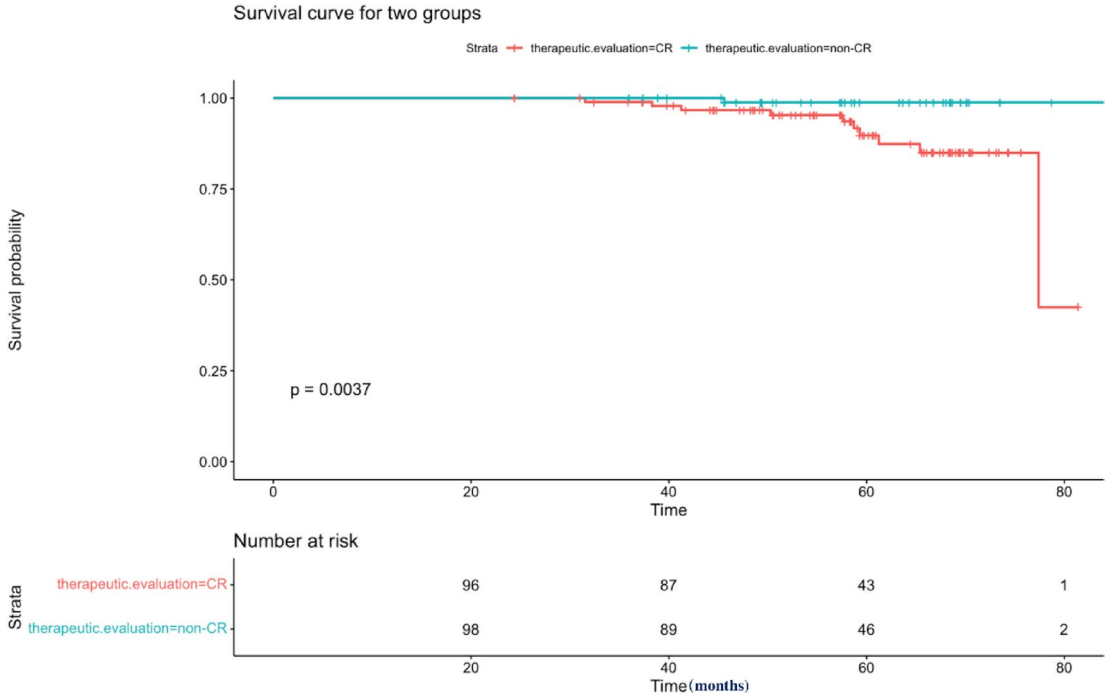

Fig. 5. The survival curves for CR group and non-CR group. the 3-year and 5-year overall survival rates of non-CR group were 100% (95%CI: 1.000 ~ 1.000) and 98.8% (95%CI: 0.9652–1.0000), respectively. The 3-year and 5-year overall survival rates of patients in CR group were 98.9% (95%CI: 0.9688–1.0000) and 89.7% (95%CI: 0.8256–0.9752), respectively, there was significant difference in two groups ($P = 0.0037$).

Assessment of the predictive abilities of three models

Decision Curve Analysis (DCA) calculates the net benefit to evaluate whether these three models are clinically useful. The results showed that the RSF model had superior predictive abilities for clinical decision-making than the DT and GBDT models both in the training and test groups (Fig. 4A,B). Therefore, Overall, the RSF model demonstrated better performance than the DT and GBDT models.

Comparison of prognosis between CR and non-CR groups

The Kaplan–Meier method from the "survminer" package in R software was used to compare the prognosis of patients with "CR" and "non-CR". The results illustrated that the 3-year and 5-year overall survival rates of non-CR group were 100% (95%CI: 1.000 ~ 1.000) and 98.8% (95%CI: 0.9652–1.0000), respectively. The 3-year and 5-year overall survival rates of patients in CR group were 98.9% (95%CI: 0.9688–1.0000) and 89.7% (95%CI: 0.8256–0.9752), respectively, there was significant difference in two groups ($P = 0.0037$) (Fig. 5).

Discussion

To our knowledge, this is the first study to use machine learning methods based on radiological dosimetric features and clinical characteristics to establish prediction model for predicting the short-term efficacy of nasopharyngeal carcinoma treatment. Currently, most assessments of short-term efficacy are based on plasma EBV levels to predict their treatment response and prognosis[20–22]. Apart from using EBV-DNA to assess efficacy, the commonly known Response Evaluation Criteria in Solid Tumors (RECIST) criteria based on imaging evaluation of solid tumor efficacy are also frequently used. However, the RECIST criteria are mainly based on post-treatment imaging to make judgments and cannot predict treatment efficacy in advance. Zeng et al.[23] used the sum of the volume regression ratio (SVRR) of the primary tumor and metastatic lymph nodes after induction chemotherapy for LANPC to compare its value in predicting patient prognosis with the treatment response based on RECIST 1.1 criteria. The results showed that SVRR was better than RECIST 1.1 in predicting the prognosis of patients after induction chemotherapy. Another study by Peng et al.[24] used deep learning methods based on PET/CT to construct a model for predicting the efficacy of induction chemotherapy for LANPC. In their results, the nomogram model built using PET/CT radiomics features achieved a C-index of 0.754 in the training group and maintained a C-index of 0.722 in the validation group, showing good consistency. Based on these previous studies, we found that the currently more mature method for predicting the efficacy of nasopharyngeal carcinoma treatment is still EBV-DNA. Therefore, we took advantage of machine learning algorithms and used three different machine learning algorithms to establish three models for predicting the short-term efficacy of LANPC, utilizing the radiological dosimetric features and clinical characteristics of NPC. In our study, we found that most of the three models incorporated radiological dosimetric features, with only one clinical feature or no clinical features included in the models, suggesting that radiological dosimetric features provided important information in predicting model outcomes. Compared to DT and GBDT models, the RSF model showed superior accuracy, sensitivity, and specificity. The features incorporated into the model include radiological dosimetric characteristics and clinical features such as PGTVnx_D95, PGTVnx_Daverage, PGTVnx_Volume, PGTVnd_R Volume, and age. The model reiterates the importance of age, the maximum prescribed dose to 95% of the primary tumor volume (D95), the volume of the primary tumor, the average dose to the primary tumor, and the volume of metastatic lymph nodes for short-term treatment efficacy, which is also consistent with current clinical consensus and research. In the results of Liao et al.[25], it was indicated that D95, D5, and homogeneity index could serve as significant dosimetric predictive indicators closely related to local recurrence, with the nasopharynx cavity, clivus, and pterygopalatine fossa identified as high-risk areas for recurrence. Moreover, D95 is a commonly used dose-volume limit prescription dose parameter in clinical practice and clinical trials[16]. In the study by Wang et al.[26] D90 was pointed out to be the key DVH characteristic for local regional recurrence in nasopharyngeal carcinoma. In ICRU Report 83[19], D50 is recommended as a dose-volume parameter for assessing IMRT plans. However, it should be noted that due to significant variability in its application across different treatment institutions and radiotherapy techniques, its clinical use requires greater caution[19,27]. In our study, we found that all three models highlighted the importance of D95 for primary nasopharynx lesions, which is consistent with the conclusions of the aforementioned studies. This underscores the significance of D95 for primary nasopharynx lesions in local tumor control. Most past research has been based on dosimetric characteristics to predict prognosis, with few scholars focusing on its impact on short-term treatment efficacy. Our study established a prediction model for short-term efficacy in locally advanced nasopharyngeal carcinoma (LANPC) by combining dosimetric and clinical characteristics. The aim is to predict the short-term efficacy of LANPC, thereby identifying high-risk patients for early intervention and also avoiding excessive treatment for some low-risk patients, providing more evidence for clinical decision-making. In our study, we not only included key dosimetric indicators but also collected information on the invasion of anatomical sites in patients with different stages. In the era of IMRT, the ability of T staging alone to divide patients into different risk groups remains weak. In the study by Wang et al.[28], it was found that in-field recurrence and high-dose region recurrence are the main patterns of local regional recurrence in NPC, with nasopharynx recurrence being the most common site, especially in patients with cervical lymph nodes larger than 3 cm, who have a higher probability of regional lymph node recurrence. Similar findings from past studies have shown that local recurrence of nasopharyngeal carcinoma is mainly concentrated in high-dose areas. In the study by Yang et al.[29], they analyzed 212 NPC patients treated with IMRT, and the results showed that 18 patients experienced recurrence, with in-field, marginal, and out-of-field recurrences accounting for 83.3%, 11.1%, and 5.6% respectively. Moreover, the areas of recurrence were primarily concentrated in high-dose regions, and expanding the CTV margins did not reduce the recurrence rate. Kong et al.[30] retrospectively analyzed 370 non-metastatic nasopharyngeal carcinoma patients who received SIB (simultaneous integrated boost) technique for the tumor region, with a total dose reaching 66–70.4 Gy. Results showed that 64% of patients experienced in-field recurrence, 12% had marginal recurrence, and 12% had out-of-field recurrence. From this study, it appears that most recurrences still occur within the treatment field. Based on the above studies, although the tumor region's dose reached more than 66 Gy, we found that there are still many patients with in-field recurrence. Therefore, we cannot help but suspect that tumors invading different anatomical sites may have varying sensitivity to radiation and thus different treatment outcomes. Hence, in our study, we included important anatomical sites and various characteristics of lymph node invasion to analyze their impact on the short-term efficacy of locally advanced nasopharyngeal carcinoma. However, among the three models we constructed, only DT model included the invasion of lateral pterygoid muscle while the other two models did not select anatomical site or lymph node characteristics as indicators affecting short-term efficacy. The reason may be that these anatomical structures are covered by different degrees of radiotherapy target volume dose according to their stage, so the results we see are basically the primary lesion or lymph nodes' radiotherapy dose, volume, or average dose, etc., included in the model as predictors of short-term efficacy. The invasion of anatomical sites or the characteristics of lymph nodes may affect prognosis more. Therefore, we have reason to believe that using the regression of anatomical invasion

structures to determine efficacy is not accurate. In the retrospective analysis by Pan et al.[31] of MRIs from 1609 nasopharyngeal carcinoma patients, the results reviewed that patients with invasion of the medial and lateral pterygoid muscles had OS similar to those with parapharyngeal space invasion. Therefore, the study suggested that the American Joint Committee on Cancer/Union for International Cancer Control (AJCC/UICC) 8th edition staging should downgrade patients with medial or lateral pterygoid muscle invasion from T4 to T2, and this recommendation was adopted. This indicates that the extent of primary tumor invasion or the status of metastatic lymph nodes significantly affects the likelihood of local recurrence or distant metastasis. Additionally, an interesting phenomenon observed in our study is that, in terms of prognosis, patients in the non-CR group had a better OS than those in the CR group. The likely reason for this could be that the tumor proliferation rate in the CR group was higher than in the non-CR group. While being more sensitive to radiation, the faster tumor growth rate may lead to a lower prognosis for the CR group compared to the non-CR group ($P = 0.0037$), which is different from the conclusion of Liu et al.[32]. Of course, there might be other reasons for this phenomenon, and further basic research analysis is needed to find the answer.

This study has three main advantages. First, it utilizes three machine learning algorithms to select features for constructing models, which can overcome the limitations of traditional statistical methods, balance the importance of various features, and avoid bias issues or data overfitting that may occur during manual data processing. Secondly, the study collected clinical and radiological dosimetric characteristics of LANPC, aiming to assess their short-term treatment efficacy rather than exploring prognostic value, which distinguishes it from other current studies. Lastly, the model constructed in this study hopes to predict patients' short-term treatment outcomes in advance, allowing for timely therapeutic interventions for high-risk patients and avoiding overtreatment for certain low-risk patients, which has significant clinical implications.

Our study also has certain limitations. First, the dosimetric characteristics collected retrospectively in this study only pertain to the maximum prescribed dose, minimum prescribed dose, average prescribed dose, and D95 for the primary lesion and metastatic lymph nodes. However, other dosimetric characteristics might also have an impact on the predictive outcomes that were not fully assessed; Second, due to the variability of past laboratory EBV-DNA level reference values, EBV-DNA levels were not included in the clinical characteristics for assessment; Finally, our model only focused on the coverage of the target volume and did not take into account the radiation doses to normal tissue organs, which is also a deficiency in our entire study. More data and multicenter collaboration will be needed in the future to validate the feasibility of the model.

Conclusion

In summary, this study constructed a prediction model for the short-term efficacy of locally advanced nasopharyngeal carcinoma using machine learning methods. This model can predict the short-term efficacy of LANPC with relatively high accuracy. Therefore, it is recommended that patients use this model at the start of treatment to predict their short-term treatment outcomes and to select individualized treatment plans.

Methods and materials

Patients and treatment

Patients diagnosed with Nasopharyngeal Carcinoma at the First Affiliated Hospital of Guangxi Medical University from January 2009 to December 2012 and at the Second Affiliated Hospital of Guangxi Medical University from January 2017 to December 2022 were retrospectively included in this study. All patients were diagnosed by histopathology as non-keratosis nasopharyngeal carcinoma. The inclusion criteria were as follows: (1) Pathologically confirmed non-keratinizing nasopharyngeal carcinoma in patients aged 18–70 years; (2) Eastern Cooperative Oncology Group (ECOG) performance score ≤2; (3) Staged III-IVa by using the 7th edition of the American Joint Committee on Cancer (AJCC) or Union for International Cancer Control (UICC) TNM staging system; (4) Patients untreated with radiotherapy or chemotherapy before; (5) No history of a second primary cancer; (6) Complete follow-up data available; (7) Pre-treatment Magnetic Resonance Imaging (MRI) imaging data available; (8)Patients treated with IMRT. The exclusion criteria were as follows: (1) Patients who have undergone surgery to remove nasopharynx tumors or biopsy of cervical lymph nodes; (2) Those without pre-treatment MRI imaging data for the nasopharynx and neck; (3) Those who did not receive radiotherapy. Clinical features collected from Medical record system include: age, gender, TNM staging, treatment modality, anatomical site involvement (including parapharyngeal space, oropharynx, prevertebral muscles, carotid sheath area, medial and lateral pterygoid muscles, cavernous sinus, skull base invasion, infratemporal fossa, nasal cavity, intracranial region, cranial nerves), lymph node status (extracapsular spread, liquefaction, necrosis, multiple confluent nodes), and areas of lymph node involvement. The Dose volume histogram (DVH) characteristics included: the Minimum Point Dose (Dmin), Maximum Point Dose (Dmax), Average Point Dose (Daverage) and Prescription Dose of 95% (D95 of) PGTVnx and PGTVnd. The DVH characteristics for each patient were directly exported from the DVH text file. Two experienced deputy directors or higher-level radiation oncologists evaluated the therapeutic efficacy of the patients' lesions at the end of radiation therapy, and at 3 months and 6 months after treatment according to the RECIST 1.1 criteria[18]. Complete response (CR) was defined as the disappearance of all target and non-target lesions on the follow-up MRI at the end of treatment, with all lymph nodes being non-pathological and < 10 mm in size. Partial response (PR) was defined as at least a 30% decrease in the sum of the diameters of the target lesions compared to baseline. Progressive disease (PD) was defined as a 20% increase in the sum of the longest diameters of the target lesions and an absolute increase of 5 mm, or the appearance of new lesions. Stable disease (SD) was defined as a reduction in the target lesions that did not meet the criteria for PR, nor an increase that met the criteria for PD. The first assessment of therapeutic efficacy was conducted at the end of radiation therapy. The study was approved by the Ethics Committee of the Second Affiliated Hospital of Guangxi Medical University.

Treatment regimens

All enrolled patients received intensity modulated radiation therapy (IMRT), which included induction chemotherapy combined with concurrent chemoradiotherapy (IC + CCRT), concurrent chemoradiotherapy (CCRT), concurrent chemoradiotherapy followed by adjuvant chemotherapy (CCRT + AC), and induction chemotherapy plus concurrent chemoradiotherapy followed by adjuvant chemotherapy (IC + CCRT + AC).

Radiation procedure

All enrolled patients were treated with intensity-modulated radiotherapy (IMRT) using a 6 MV-X linear accelerator on one daily fraction of 5 days per week. Treatment planning systems (TPS) used were either Varian 2.0, Eclipse 13.6 or Pinnacle. Contouring of the target volumes was performed in accordance with the principles outlined in International Commission on Radiological Protection (ICRU) Report 83[19]. Prescription dose: Planning gross Target Volume of nasopharynx (PGTVnx) 70~73 Gy/31-33f, Planning gross Target Volume of lymph nodes (PGTVnd) 66~70Gy/31-33f, Planning high risk tumor volume (PTV1) 60–64 Gy/28-33f, Planning low risk tumor volume (PTV2) 54–56 Gy/28–33 f. Normal tissue constraints were based on the Radiation Therapy Oncology Group (RTOG) 0225 protocol[16]. Dosimetric parameters for each patient were derived from the DVH, including maximum point dose of the target (Dmax), mean dose of the target (Dmean), minimum point dose of the target (Dmin), maximum dose to 1 cubic centimeter (D1cc), and the minimum absorbed dose that covers 95% of the target volume (D95).

Chemotherapy regimens

Induction chemotherapy

TPF: docetaxel : 60 mg/m2/d1,DDP:60 mg/m2/d1,5-fluorouracil: 600 mg/m2/d1-5, continuous intravenous infusion over 120 h or intravenous drip; GP: gemcitabine:1 g/m2/d1,DDP:80 mg/m2/d1; TP: docetaxel : 75 mg/m2/d1,DDP:75 mg/m2/d1;every three weeks for two to three cycles.PF: DDP:80 mg/m2/d1,5-fluorouracil:750 mg/m2/d1-5, continuous intravenous infusion over 120 h or intravenous drip, every four weeks for two to three cycles.

Concurrent chemotherapy

DDP:100 mg/m2/d1,every three weeks for two to three cycles or DDP: 40 mg/m2/d1,every week for six to seven cycles.

Adjuvant chemotherapy

PF: DDP:80 mg/m2/d1,5-fluorouracil:750 mg/m2/d1-5, continuous intravenous infusion over 120 h or intravenous drip, every four weeks for two to three cycles. TP: docetaxel: 75 mg/m2/d1, DDP:75 mg/m2/d1, every three weeks for two to three cycles.

Radiological dosimetry features

Radiodosimetric analysis included the PGTVnx, left cervical lymph node tumor volume (PGTVnd-L), and right cervical lymph node tumor volume (PGTVnd-R). The DVH of the enrolled patients were exported from Pinnacle or Eclipse treatment planning systems (Eclipse 13.6). The parameters provided by the DVH included the Dmax, Dmin, Daverage, variable volume (volume), and D95. Table 2 showed more details.

Follow-up

After the completion of treatment, patients were followed up every three months for the first two years, every six months from the third to fifth year, and annually thereafter.

Methods of machine learning

Decision tree model (DT model)

Using the "rpart" package in R version 4.2.1, patients were randomly divided into a training group and a test group at a ratio of 7:3, with 70% allocated to the training set ($n = 137$) and 30% to the test group ($n = 57$).

The "ROSE" package in R version 4.2.1 was used to balance the data of the training and test groups according to the efficacy evaluation, in order to enhance the practicality and accuracy of the model. The complexity parameter (cp.) value was set to 0.01 to obtain the original classification tree. Then, based on the minimum cross-validation error of the complexity parameter, the cp. value was adjusted to 0.0066 for post-pruning of the model. Subsequently, the original classification tree was obtained, which allowed for the assessment of the importance of each variable. DT model was constructed based on the results of the post-pruning. Using the "pROC" package in R software, the sensitivity, specificity, and accuracy of the model in the training and test cohort were obtained, along with the ROC curve and AUC value for the model.

XGBoost decision model (GBDT model)

The "XGBoost" package in R version 4.2.1 was used for data analysis and model construction. GBDT model was built by reducing different weights according to the varying importance of each feature. The "pROC" package in R software was employed to determine the sensitivity, specificity, and accuracy of the model in both the training and test groups, as well as to obtain the ROC curve and AUC value for the model.

Random forest model (RSF model)

The RSF model was constructed using the "randomForest" package in R version 4.2.1 software based on the training dataset. The training dataset was generated using random bootstrapping. To minimize classification error in the training data, the model randomly selected a subset of feature variables (m_{try}) to obtain optimal

results. Trees corresponding to the training set were repeatedly generated until the out-of-bag (OOB) error rate stabilized. Subsequently, the RSF model selected the one with the lowest OOB error rate. Using the "pROC" package to obtained the sensitivity, specificity, and accuracy of the model in both the training and test groups, as well as the ROC curve and AUC value for the model. On the basis of the RSF model, the log-rank test was performed on patients with efficacy evaluations of CR and non-CR group using the Kaplan–Meier method from the "survminer" package. Survival curves for both groups of patients were also plotted.

Calculation of area under ROC curve

The Receiver Operating Characteristic (ROC) curve was used to assess the predictive accuracy of different models (DT, GBDT and RSF models). The Area Under the Curve (AUC) of the ROC was used as a performance metric for all models. The "pROC" package in R was utilized to obtain the ROC curves and AUC values, with the AUC values being calculated to compare the discriminative abilities of the three models.

Comparison the prognosis of patients with different therapeutic responses

By comparing the ROC curves and AUC values of the three models, the RSF model provided the best accurate predictive results. Using the "survminer" package and the log-rank test with the Kaplan–Meier method, we compared the survival rates of patients in the CR and non-CR groups and presented the Kaplan–Meier survival curves for both groups, evaluating the prognosis of the patients in these two groups.

Statistical analysis

Categorical variables were analyzed by the Pearson $\chi 2$ test, and continuous variables were assessed with the Mann–Whitney U test to determine significant differences between the training and test groups. DVH features were exported from the planning system. All statistical analyses and figures were performed using R version 3.6.1. The Receiver Operating Characteristic (ROC) curve was employed to evaluate the predictive accuracy of different efficacy prediction models. The Area Under the Curve (AUC) of the ROC was used as a performance metric for all models, with AUC values utilized to compare the discriminative abilities of the mentioned models. The Kaplan–Meier method was used to compare survival curves between CR and non-CR group. A p-value of < 0.05 was considered statistically significant. All tests were two-sided with a 95% confidence interval. The flow chart was shown in Fig. 6.

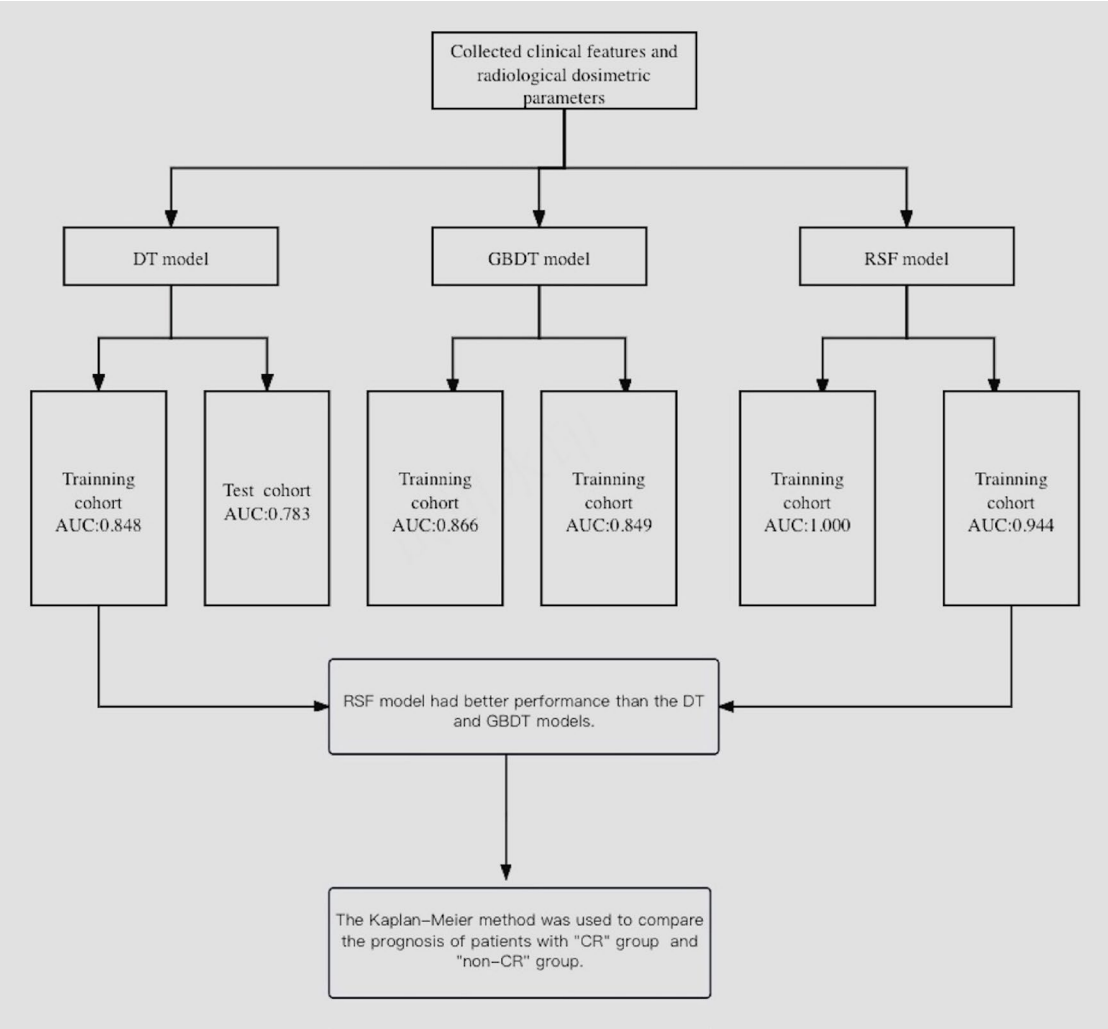

Fig. 6. The flow chart of the study.

Data availability

All patient data from this study are kept private to protect patient confidentiality, but can be made available from the corresponding author on reasonable request.

Received: 4 October 2024; Accepted: 16 May 2025
Published online: 21 May 2025

References

1. Tian, Y. M. et al. Long-term outcome and pattern of failure for patients with nasopharyngeal carcinoma treated with intensity-modulated radiotherapy. *Head Neck*. **41** (5), 1246–1252. https://doi.org/10.1002/hed.25545 (2019).
2. Tang, L. L. et al. The Chinese Society of Clinical Oncology (CSCO) clinical guidelines for the diagnosis and treatment of nasopharyngeal carcinoma. *Cancer Commun. (Lond)* **85**, 68–69 (2023).
3. Sun, Y. et al. Induction chemotherapy plus concurrent chemoradiotherapy versus concurrent chemoradiotherapy alone in locoregionally advanced nasopharyngeal carcinoma: a phase 3, multicentre, randomised controlled trial. *Lancet Oncol.* **17** (11), 1509–1520. https://doi.org/10.1016/S1470-2045(16)30410-7 (2016).
4. Chen, Y. P. et al. Chemotherapy in combination with radiotherapy for Definitive-Intent treatment of stage II-IVA nasopharyngeal carcinoma: CSCO and ASCO guideline. *J. Clin. Oncol.* **39** (7), 840–859. https://doi.org/10.1200/JCO.20.03237 (2021).
5. Pfister, D. G. et al. Head and neck cancers, version 2.2020, NCCN clinical practice guidelines in oncology. *J. Natl. Compr. Canc Netw.* **18** (7), 873–898. https://doi.org/10.6004/jnccn.2020.0031 (2020).
6. Zhang, Y. et al. Gemcitabine and cisplatin induction chemotherapy in nasopharyngeal carcinoma. *N Engl. J. Med.* **381** (12), 1124–1135. https://doi.org/10.1056/NEJMoa1905287 (2019).
7. Sengar, M. et al. Cell-free Epstein-Barr virus-DNA in patients with nasopharyngeal carcinoma: plasma versus urine. *Head Neck*. **38** (Suppl 1), E1666–E1673. https://doi.org/10.1002/hed.24297 (2016).
8. Chan, A. T. et al. Plasma Epstein-Barr virus DNA and residual disease after radiotherapy for undifferentiated nasopharyngeal carcinoma. *J. Natl. Cancer Inst.* **94** (21), 1614–1619. https://doi.org/10.1093/jnci/94.21.1614 (2002).
9. Lin, J-C. et al. Quantification of plasma Epstein–Barr virus DNA in patients with advanced nasopharyngeal carcinoma. *N Engl. J. Med.* **350** (24), 2461–2470 (2004).

10. Prayongrat, A., Chakkabat, C., Kannarunimit, D., Hansasuta, P. & Lertbutsayanukul, C. Prevalence and significance of plasma Epstein-Barr virus DNA level in nasopharyngeal carcinoma. *J. Radiat. Res.* **58** (4), 509–516 (2017).
11. Peng, H. et al. Prognostic impact of plasma Epstein-Barr virus DNA in patients with nasopharyngeal carcinoma treated using intensity-modulated radiation therapy. *Sci. Rep.* **6**, 22000 (2016).
12. Twu, C.-W. et al. Comparison of the prognostic impact of serum anti-EBV antibody and plasma EBV DNA assays in nasopharyngeal carcinoma. *Int. J. Radiat. Oncol. Biol. Phys.* **67**(1), 130–137 (2007).
13. Chan, A. T. C. et al. Analysis of plasma Epstein-Barr virus DNA in nasopharyngeal Cancer after chemoradiation to identify High-Risk patients for adjuvant chemotherapy: A randomized controlled trial. *J. Clin. Oncol.* **36** (31), 3091–3100 (2018).
14. Chan, A. T. C. et al. Plasma Epstein-Barr virus DNA and residual disease after radiotherapy for undifferentiated nasopharyngeal carcinoma. *J. Natl. Cancer Inst.* **94** (21), 1614–1619 (2002).
15. Jiang, Y. et al. A dynamic nomogram combining tumor stage and magnetic resonance imaging features to predict the response to induction chemotherapy in locally advanced nasopharyngeal carcinoma. *Eur. Radiol.* **33** (3), 2171–2184. https://doi.org/10.1007/s00330-022-09201-8 (2023).
16. Lee, N. et al. Intensity-modulated radiation therapy with or without chemotherapy for nasopharyngeal carcinoma: radiation therapy oncology group phase II trial 0225. *J. Clin. Oncol.* **27**, 3684–3690 (2009).
17. Jiang, Y. T. et al. A nomogram to predict survival and guide individualized induction chemotherapy in T3-4N1M0 nasopharyngeal carcinoma. *Curr. Probl. Cancer*. **46** (6), 100897. https://doi.org/10.1016/j.currproblcancer.2022.100897 (2022). Epub 2022 Sep 19.
18. Eisenhauer, E. A. et al. New response evaluation criteria in solid tumours: revised RECIST guideline (version 1.1). *Eur. J. Cancer*. **45** (2), 228–247. https://doi.org/10.1016/j.ejca.2008.10.026 (2009).
19. Hodapp, N. & Der, I. C. R. U. R. 83: Verordnung, Dokumentation und Kommunikation der fluenzmodulierten Photonenstrahlentherapie (IMRT) [The ICRU Report 83: prescribing, recording and reporting photon-beam intensity-modulated radiation therapy (IMRT)]. *Strahlenther Onkol.* **188**, 97–99. https://doi.org/10.1007/s00066-011-0015-x (2012).
20. Zhou, H. et al. Effects of oral maintenance chemotherapy and predictive value of Circulating EBV DNA in metastatic nasopharyngeal carcinoma. *Cancer Med.* **9** (8), 2732–2741. https://doi.org/10.1002/cam4.2926 (2020).
21. Chen, F. P. et al. Circulating Epstein-Barr virus DNA level post induction chemotherapy contributes to prognostication in advanced-stage nasopharyngeal carcinoma. *Eur. J. Cancer*. **151**, 63–71. https://doi.org/10.1016/j.ejca.2021.03.052 (2021).
22. Zhang, W. et al. The clinical utility of plasma Epstein-Barr virus DNA assays in nasopharyngeal carcinoma: the dawn of A new era? A systematic review and meta-analysis of 7836 cases. *Med. (Baltim).* **94** (20), e845. https://doi.org/10.1097/MD.0000000000000845 (2015).
23. Zeng, Y. Y. et al. The comparison of prognostic value of tumour volumetric regression ratio and RECIST 1.1 criteria after induction chemotherapy in locoregionally advanced nasopharyngeal carcinoma. *Oral Oncol.* **111**, 104924. https://doi.org/10.1016/j.oraloncology.2020.104924 (2020).
24. Peng, H. et al. Prognostic value of deep learning PET/CT-Based radiomics: potential role for future individual induction chemotherapy in advanced nasopharyngeal carcinoma. *Clin. Cancer Res.* **25** (14), 4271–4279. https://doi.org/10.1158/1078-0432.CCR-18-3065 (2019).
25. Liao, W. et al. A novel dosimetric metrics-based risk model to predict local recurrence in nasopharyngeal carcinoma patients treated with intensity-modulated radiation therapy. *Radiat. Oncol.* **16** (1), 186. https://doi.org/10.1186/s13014-021-01911-5 (2021).
26. Wang, J. et al. The impact of target dosimetry on patients' locoregional recurrence in nasopharyngeal carcinoma: A propensity score-matched analysis. *Radiother Oncol.* **141**, 67–71 (2019).
27. Das, I. J. et al. State of dose prescription and compliance to international standard (ICRU-83) in intensity modulated radiation therapy among academic institutions. *Pract. Radiat. Oncol.* **7**(2), e145–e155. https://doi.org/10.1016/j.prro.2016.11.003 (2017).
28. Wang, L. et al. Clinical analysis of recurrence patterns in patients with nasopharyngeal carcinoma treated with Intensity-Modulated radiotherapy. *Ann. Otol. Rhinol. Laryngol.* **126**(12), 789–797. https://doi.org/10.1177/0003489417734229 (2017).
29. Yang, X. et al. Analysis of clinical target volume delineation in Local-regional failure of nasopharyngeal carcinoma after Intensity-modulated radiotherapy. *J. Cancer*. **11** (7), 1968–1975. https://doi.org/10.7150/jca.39588 (2020).
30. Kong, F. et al. Patterns of local-regional failure after primary intensity modulated radiotherapy for nasopharyngeal carcinoma. *Radiat. Oncol.* **9**, 60. https://doi.org/10.1186/1748-717X-9-60 (2014).
31. Pan, J. J. et al. Proposal for the 8th edition of the AJCC/UICC staging system for nasopharyngeal cancer in the era of intensity-modulated radiotherapy. *Cancer* **122** (4), 546–558. https://doi.org/10.1002/cncr.29795 (2016).
32. Liu, X. et al. Nomograms incorporating primary tumor response at mid-radiotherapy to predict survival in locoregionally advanced nasopharyngeal carcinoma. *Head Neck*. **45** (8), 1922–1933 (2023).

Acknowledgements

This work was finished by the team of Department of Radiation Oncology, the Second Affiliated Hospital of Guangxi Medical University and the Guangxi Medical University cancer hospital, and Thank you for all my colleagues.

Author contributions

Conceptualization and study design: Jian Li and Xiaodong Zhu. Data verification: Jiaying Wen, Qianfu Liang, Danjing Luo. Funding acquisition: Jian Li, Haiying Yue and Jiaying Wen. Project administration: Xiangde Li, Qiulu Zhong. Supervision: Xiaodong Zhu, Wenqi Liu, Jian Li and Haiying Yue. Methodology: Qiulu Zhong and Xiangde Li. Investigation: Qiulu Zhong, Qinghua Du, Danjing Luo and Jiaying Wen. Validation: Qiulu Zhong, Qinghua Du, Danjing Luo. Original draft, and writing: Qiulu Zhong and Xiangde Li. Final approval of the manuscript: All the authors.

Funding

This work was supported by the grants from the project of the Guangxi Suitable Technology Development and Promotion Application Project (No. S2017013), the Youth Science Foundation of Guangxi Medical University (No. GXMUYSF202423), the Guangxi Health Commission's Medical and Health Self-financed Project (No. Z20190059).

Declarations

Competing interests

The authors declare no competing interests.

Ethics approval and consent to participate

The study was approved by the Ethics Committee of the Second Affiliated Hospital of Guangxi Medical University. The requirement for informed consent was waived by the ethics committee/Institutional Review Board of the Second affiliated Hospital of Guangxi Medical University. All methods were performed in accordance with the relevant guidelines and regulations.

Consent for publication

Not applicable.

Additional information

Correspondence and requests for materials should be addressed to X.Z. or J.L.

Reprints and permissions information is available at www.nature.com/reprints.

Publisher's note Springer Nature remains neutral with regard to jurisdictional claims in published maps and institutional affiliations.